JOURNAL OF OPTOELECTRONICS AND ADVANCED MATERIALS Vol. 12, No. 11, November 2010, p. 2255 - 2260

Microwave synthesis, optical, structural and magnetic characterization of ZnO/Mn doped ZnO nanoparticles

A. K. SINGH
Nanomaterials and Sensors Lab., Defence Institute of Advanced Technology (Deemed University), Girinagar, Pune-411025, Maharashtra, India.

Paper reports the synthesis of ZnO/Mn doped ZnO nanoparticles via microwave method using Zinc Acetate, Manganese Acetate in de-ionized (DI) water and Polyvinlypyrolidone (PVP) as a capping agent. X-ray diffraction (XRD), Scanning electron microscopy (SEM) and Energy dispersive X-ray (EDAX) is used for structural and morphological characterization of ZnO/Mn doped ZnO nanoparticles. Particle size has been calculated using effective mass approximation method from UV-VIS spectroscopy and Scherrer's formula from XRD patterns which is in good agreement with the result obtained from SEM. XRD analysis reveal single crystal ZnO/Mn doped ZnO nanoparticles of size 10-59 nm. Effect of capping agent on the particle size of the ZnO has been studied using UV-VIS and particle size analyzer. PL of ZnO/Mn doped ZnO sample has beeen also recorded at room temperature with excitation wavelength 325 nm. Sharp ultraviolet emission of the band edge luminescence has been observed at 3.27 eV (380 nm) in case of ZnO whereas peak emission has been observed at 3.2059 eV (387 nm) in case of Mn doped ZnO nanoparticles. VSM of synthesized Mn doped ZnO nanoparticles annealed at 527 K for 9 hrs has been investigated at room temperature and ferromagnetic behavior is observed.

(Received October 12, 2010; accepted November 19, 2010)

Keywords: Micro wave synthesis, Mn doped ZnO, UV-Vis, SEM, photoluminescence, VSM

1. Introduction

Nanoscale semiconductor materials has been extensively studied in manufacturing electronic and optoelectronic devices [1-5]. ZnO being direct band gap semiconductor has high exciton binding energy (60 meV) would allow excitonic transitions at room temperature, meaning high radiative recombination efficiency for spontaneous emission as well as lower threshold voltage for emission. ZnO is considered as a substitute to GaN and ITO, as transparent conducting oxide. It has high electrochemical stability and control over resistance (10^{-3} to 10^{-5} Ω). It is therefore a potential candidate for optoelectronic applications in the short wavelength range (green, blue, UV), information storage and sensors [6-11]. Recently, diluted magnetic semiconductors (DMSs) have attracted wide attention because in these materials new functions can be added by transporting and controlling various types of spin states. Much of the recent effort toward spintronics has been focused on manganese doped III-V and II-VI materials, with prominent interest in GaN:Mn and ZnO:Mn. One of the major challenges lies in preparing a ferromagnetic material having Curie temperature above room temperature. Interest is focused on ZnO doped with 3*d* transition metals. ZnO plays an important role in the field of DMSs. The transition metal doped ZnO has the potential to be highly multifunctional material with coexisting magnetic, semiconductor, electromechanical and optical properties. From theoretical considerations it is predicted that ZnO doped with 5 at.%Mn^{2+} and containing 3.5×10^{20} holes/cm^3 may exhibit ferromagnetism with *T*C > RT [12]. A number of researcher have therefore investigated the ferromagnetic properties on Mn doped ZnO in the last few years. While some authors claimed to have evidence of the existence of room-temperature ferromagnetism in ZnMnO, others detected anti-ferromagnetic or paramagnetic [13-17] behavior in this material. Most groups observe ferromagnetism at low temperatures. Some researchers have found ferromagnetism above room temperature for transition-metal-doped ZnO [18] and in thin films made under non-equilibrium conditions [9, 19].

Most Mn-doped ZnO samples are grown employing complex and expensive techniques like molecular beam epitaxy, metalorganic vapor phase epitaxy or pulsed laser deposition that require high growth temperatures. In contrast to these methods, cost effective large scale production methods are required. Recently, microwave irradiation has been widely applied to material science. Due to intense friction and the collision of molecules created by microwave irradiation, microwave irradiation not only provides the energy for heating but also greatly accelerates the nucleation. With microwave irradiation on the reactant solution, temperature and concentration gradients can be avoided leading to uniform nucleation. Microwave-based synthesis method is one of the easiest, energy-saving, and quick methods for largescale production of nanomaterials[20]. The ability of PVP as reducing agent has been reported by various researchers [20]. The dispersion and diameters of nanoparticles is greatly influenced by the ratio between reactants, amount of PVP, the reaction time, and reaction temperature. Further, a doping technique for the synthesis of nanosized structures is also to be established.

In this paper, we report ferromagnetic behavior of Mn doped ZnO nanoparticles and also device a simple method for the preparation of hexagonal ZnO/Mn doped ZnO nanoparticles using microwave irradiation. Particles obtained by this method are of good quality and high crystallinty.

2. Experimental

2.1 Instrumentation and preparation

A microwave oven with 700 watt power is used for preparing ZnO/Mn doped ZnO nanoparticles. X-ray diffraction (XRD) patterns of prepared samples are recorded by X-ray diffractometer (XRD Panalytical-Xpert Pro.) using a CuK_α radiation (λ=1.54A^0). The morphology and elemental analysis is examined by a (JEOL ASM 6360 A) SEM. A nanodrop 1000 UV-Vis spectrometer is used to record the UV visible absorption spectra with 1mm column. PSS-NICOMP particle sizing system is used for particle size determination, Alba F CS^{TM} & Chronos BH^{TM} is used for recording PL and magnetic behaviour of sample is studied using vibrating sample magnetometer (VSM) Lake Shore 7307 model.

To prepare ZnO nanoparticles 25ml aqueous solution of 0.2M zinc acetate is mixed with 25 ml aqueous solution of 0.4 M sodium hydroxide. PVP (PVP to zinc acetate in different proportions i.e. ¼, ½, 1, 2, 3, 5, 10) is added to the prepared solution to see the effectiveness of PVP and the mixture is placed under microwave irradiation at temperature 60 ^oC. The precipitate formed is separated from the solution by filtration, washed several times with DI water and absolute ethanol, and then dried in an oven to obtain nanocrystalline powder. Similarly to prepare 5% Mn doped ZnO, two solutions, one containing zinc acetate di hydrate 45mmol and the other containing manganese acetate tetra hydrate 2.4mmol in 200ml of DI water, are prepared and kept under microwave treatment at 60 ^oC. Another solution of KOH 140 mmol in 200ml DI water is prepared and added drop by drop to the above solution while stirring at room temperature. The precipitate which gets formed is separated from the solution by filtration, washed several times with DI water and absolute ethanol, and then dried in oven to obtain Mn doped ZnO nanocrystalline powder.

3. Results and discussion

3.1 Scanning electron microscopy & energy dispersive analysis of X-ray (SEM & EDAX)

The SEM of ZnO/Mn doped ZnO in Fig. 1 shows the morphology and size distribution of particles. As seen, in case of ZnO/Mn doped ZnO, single phase primary particle, spherical in shape of average size (diameter) of about 50 nm gets formed.

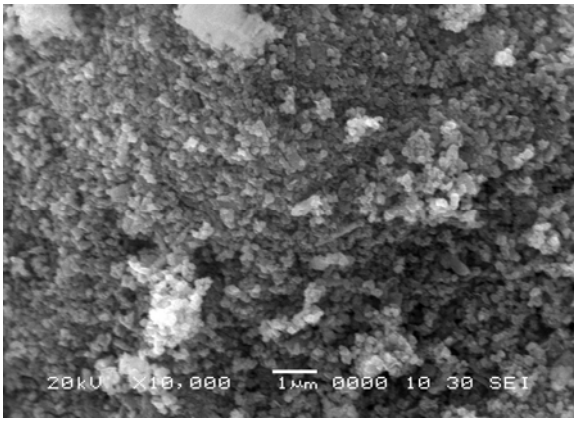

a

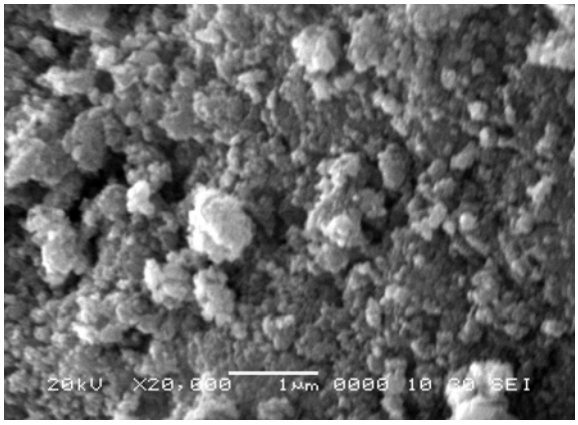

b

Fig. 1. SEM of (a) ZnO nanoparticles (b) Mn doped ZnO nanoparticles.

Stoichiometry of ZnO/ Mn doped ZnO nanoparticles, confirmed by EDAX elemental analysis and is shown in Fig. 2. The results indicate formation of high purity ZnO/Mn doped ZnO nanoparticles.

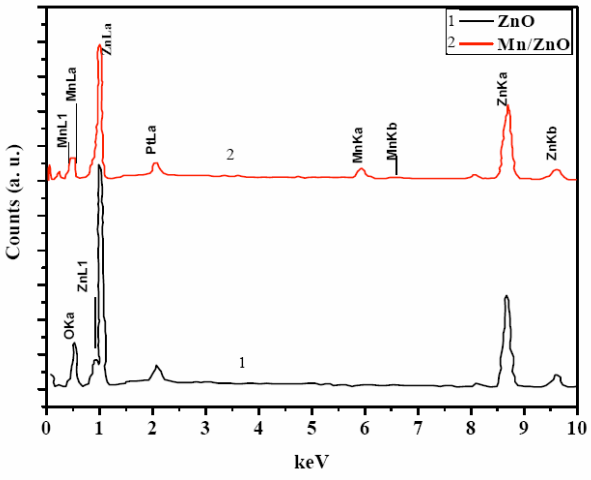

Fig. 2.The EDAX analysis of ZnO nanopowder & 5% Mn doped ZnO nanopowder.

3.2 X-ray diffraction (XRD)

Fig. 3 shows the XRD pattern of ZnO/Mn doped ZnO nanoparticles. The obtained diffraction pattern is compared with JCPDS data sheet JCPDS-080-0074. The characteristic peaks with high intensities corresponding to the planes (100), (002), (101), (102), (110), (200), (112) and (201) indicate the product is of high purity hexagonal ZnO wurtzite structure. It is evident from the XRD data that there are no extra peaks due to manganese metal, other oxides or any zinc manganese phase, indicating that the as-synthesized samples are single phase. But in comparison to the diffraction pattern of the un-doped sample, the peak positions of the ZnO : Mn sample has shifted towards smaller angles and thus indicating the increase in lattice constants, as shown in Table1, i.e. incorporation of Mn inside the ZnO crystal lattice [12]. Previous studies of manganese-doped ZnO have taken the observed lattice parameter expansion as evidence for the doping of Mn cation into ZnO [11].

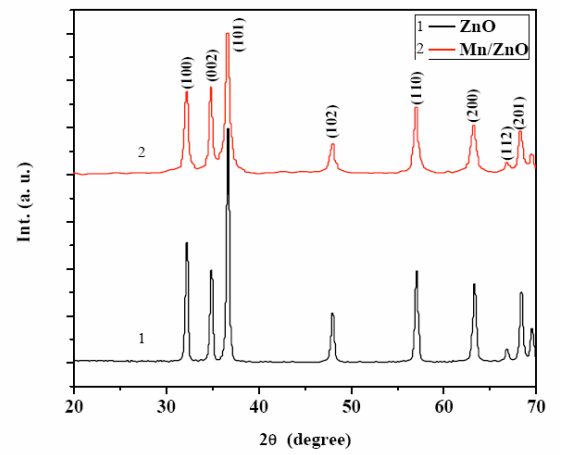

Fig. 3. X-ray diffraction pattern of (a) ZnO and Mn doped ZnO (b) Enlarge view of X-ray diffraction pattern between 30 to 40 angles for ZnO and Mn doped ZnO.

Table 1. Blue shift in the diffraction peaks for ZnO/ Mn doped ZnO.

No.	(hkl)	2θ (degree)		Shift Observed (degree)
		Pure ZnO	Mn doped ZnO	
1.	(100)	32.1981	32.1540	0.0441
2.	(002)	34.8166	34.7608	0.0558
3.	(101)	36.6905	36.5690	0.1215
4.	(102)	47.9751	47.9073	0.0678
5.	(110)	57.0114	56.9789	0.0325
6.	(200)	63.2546	63.2454	0.0092
7.	(112)	66.7321	66.7237	0.0084
8.	(201)	68.3431	68.2610	0.0821

The peaks at various scattering angles (2θ) are used to calculate the particle size using Scherrer's formula:

$$d = 0.9\lambda/\beta\cos\theta \qquad (1)$$

where d is the particle size, λ is the wavelength of X- ray, β is the measured FWHM (full-width at half maximum), θ is the Bragg peak angle of the peak. The average particle size estimated from the above formula is in the range from 10 nm-60 nm for ZnO and 50-100 nm for Mn doped ZnO. This is in agreement with the average size obtained from SEM. The crystallite sizes obtained indirectly by XRD and directly by electron microscopy may not always exactly match. Whereas the electron microscopy can be used to determine almost any crystallite size, X-ray peak broadening methods give the most correct results for crystallite sizes in the range of 10–100 nm [21].

3.3 UV-VIS spectroscopy

Fig. 4 shows the UV absorption spectra of ZnO for different PVP to zinc acetate ratio. The absorption spectra for all the samples are blue shifted from 375 nm (expected for bulk ZnO having direct band gap of 3.3 eV) which confirms the formation of ZnO nanoparticles. Excitonic absorption peak observed are very sharp indicating monodispersed nature of the nanoparticles distribution which is also confirmed by PSS. No observable change in particle size is found for different PVP to zinc acetate ratio from the PSS, however absorption peak has been found slightly blue from 357 nm to 353 nm for three times PVP to Zinc acetate ratio and further increase in PVP above two times has been ineffective (results are shown upto three times).

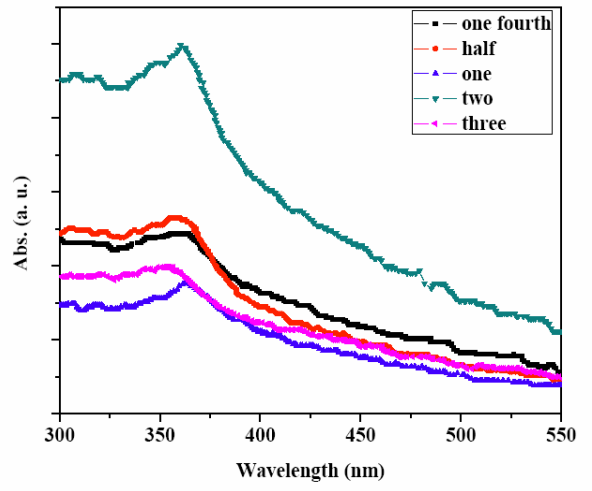

Fig. 4. UV-Vis absorption spectra of ZnO nanoparticles for different PVP to zinc acetate ratio.

Following equation is used to calculate the particle size (radius)

$$r\,(nm) = \frac{-0.3049 + \sqrt{-26.23012 + \frac{10240.72}{\lambda_p(nm)}}}{-6.3829 + \frac{2483.2}{\lambda_p(nm)}} \qquad (2)$$

Above equation is derived using the effective mass model [22] which describe the particle size (r, radius) as a function of peak absorbance wavelength (λp) for ZnO nanoparticles.

Particle sizing system(PSS), based on the principal of dynamic light scattering(DLS) is also used to find out the size of ZnO nanoparticles of different PVP to zinc acetate ratio. Two different curves: volume weight and number weight are used to determine the particle size, showing similar particle size distribution. The average size obtained from the PSS is about 10-15 nm as shown in Fig. 5 which is in agreement with the result obtained from UV-VIS using equation (2). Here only a set of results are shown for particle size distribution. The summary of results is presented in Table 2.

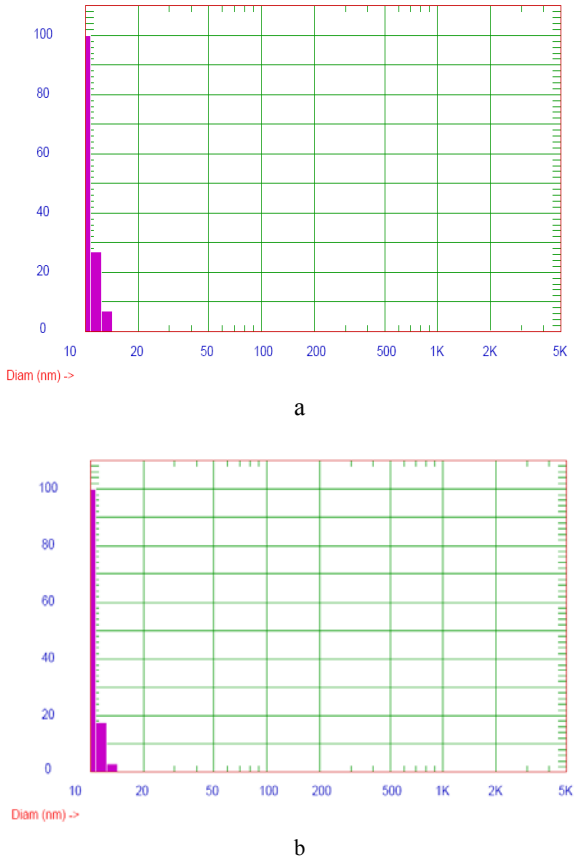

Fig. 5. Particle size distribution of prepared ZnO nanoparticles based obtained from PSS based (DLS) using (a) Volume-weight distribution (b) Number-weight distribution for ZnO nanoparticles.

Table 2. Summary of ZnO synthesis results, effect of capping agents on UV absorption peak and particle size.

No	Capping agent	Quantity of capping agent	UV absorption peak	Size of particles obtained
1	PVP	One fourth of Zinc acetate	357	4-5 nm
2	PVP	Half of Zinc acetate	357	4-5 nm
3	PVP	One time of Zinc acetate	357	4-5 nm
4	PVP	Two times of Zinc acetate	354	4-5 nm
5	PVP	Three times of Zinc acetate	353	4-5 nm

3.4 Photoluminescence (PL)

Fig. 6 shows the PL spectrum of the ZnO/Mn doped ZnO nanopowder at room temperature excitated at wavelength 325 nm. Sharp ultraviolet emission has been observed at 3.27 eV (380 nm) in case of ZnO whereas peak emission has been observed at 3.2059 eV (387 nm) in case of Mn doped ZnO nanoparticles and low intensity peak at 3.0 eV (410 nm) in both samples. This peak at 410 nm is attributed to zinc vacancies [23]. UV emission

corresponds to the near band edge emission of the wide band gap of ZnO because of annihilation of excitons and quantum confinement [23]. No additional peak is observed due to the presence of Mn. Additional signal peak from the implanted Mn ions has been not expected, because Mn does not form any acceptor or donor levels within ZnO [24]. Mn doped ZnO Pl peak intensity is more than one order of magnitude less than the signal observed for pure ZnO. The PL suppressed intensity with Mn is in accordance with earlier literature reports [21, 24].

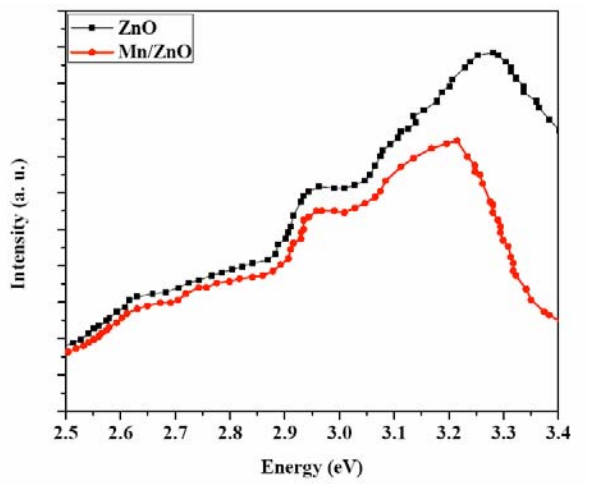

Fig. 6. Photoluminescence spectrum of ZnO/Mn doped ZnO nanopowders at room temperature excited at wavelength 325 nm.

3.5 Vibrating sample magnetometer (VSM)

Magnetic property of Mn doped ZnO samples using VSM at the room temperature annealed at 527K for 9 hrs. has been studied and results are shown in Fig. 7. The field dependence of the magnetization (M versus H) curve at 303K shows clear hysteresis loops for the Mn doped ZnO sample with PVP and without PVP. Mn doped sample with PVP shows larger magnetization and an eblarged view is shown in the window of Fig. 7. Both the curves show ferromagnetic behavior at room temperature. It can be considered that the ferromagnetic coupling essentially is due to the Mn atoms in both the irregularly shaped and the hexagonally shaped particles. These results confirm that Mn doping into ZnO lattice induce ferromagnetic ordering at room temperature[25], which can be attributed to the substitutional incorporation of Mn at Zn-sites[13]. The small coercivity and the small area under the hysteresis loop characterize these materials as soft ferromagnets and these observations are consistent with those reported for other ferromagnetic ZnO and nanocrystalline DMS aggregates [26-27].

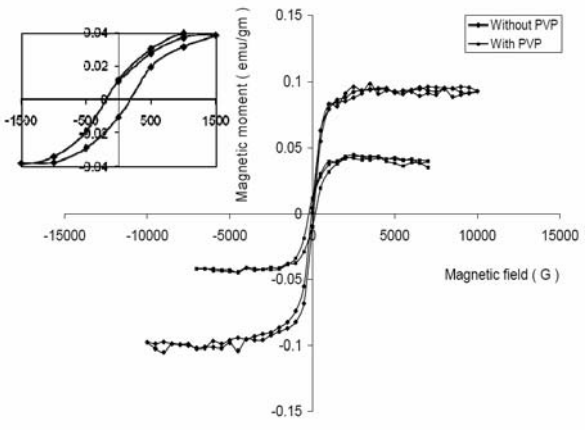

Fig. 7. M versus H curves at 303 K for the Mn-doped ZnO sample annealed at 527 K for 9 h with PVP and without PVP (Enlarge view of Mn doped ZnO with PVP is also shown).

4. Conclusions

ZnO/ Mn doped ZnO nanoparticles have been prepared by microwave irradiation method using zinc acetate, manganese acetate, DI water and PVP. The samples were characterized using X-ray diffraction, SEM, EDAX techniques. The important findings are as follows:

1) Microwave irradiation method has been found to be an easy, very fast and environmental friendly compared to other methods.
2) No significant change has been observed in particle for different amount of capping agent used during synthesis.
3) PL spectra shows no additional peak due to doping of Mn in ZnO.
4) Ferromagnetic ordering has been observed at room temperature in Mn doped ZnO sample annealed at 527 K.

Acknowledgments

Authors are thankful to Vice-Chancellor, DIAT, Pune for granting permission to publish this work. Authors would like to thank Department of Physics, University of Pune for providing Photoluminescence, SEM, EDAX and VSM facility and Director HEMRL Pune for XRD of samples.

References

[1] M. K. Patra, K. Manzoor, M. Manoth, S.R. Vandera, N. Kumar, J. Lumines. **128**, 267 (2008).
[2] P. Kumbhakar, D. Singh, C.S. Tiwary, A.K. Mitra, Chalcogenide Lett. **5**(12), 387 (2008).

[3] L.W. Zhong, J. Song, Science **312**, 242 (2006).
[4] S. J. Pearton, D. P. Norton, K. Ip, Y.W. Heo, T. Steiner, Prog. Mat. Sci. **50**, 293 (2005).
[5] Y. K. Xiang, L.W. Zhong, Nanolett. **3**(12), 1625 (2003).
[6] M. Jayalakshmi, M. Palaniappa, B. Balasubramanian, Int. J. Electrochem. Sci. **3**, 96 (2008).
[7] L. Lie, Y. Zhang, S.S. Mao, L. Lin, Sens, Actuat.:A **127**, 201(2006).
[8] H. Hayashi, A. Ishizaka, M. Haemori, H. Kinuma, Appl. Phys. Lett. **82**, 1365 (2003).
[9] X. M. Cheng, C.L. Chein, J. Appl. Phys. **93**, 7876 (2003).
[10] P. Sharma, K. Sreenivas, K.V. Rao, J. Appl. Phys. **93**, 3963 (2003).
[11] T. Takuya, Z. Smith, P. Andrew, R. He, X. Wang, J. Austral. Ceram. Soc. **45**(1), 58(2009).
[12] E. Schlenker, A. Bakin, H. Schmid, W. Mader, H. Bremers, A. Hangleiter, H.H.Wehmann, M. Al-Suleiman, J. L ¨Udke, M. Albrecht, A. Waag, **91**(3), 375(2008).
[13] O. D. Jayakumar, H. G. Salunke, R. M. Kadam, M. Mohapatra, G. Yaswant, S. K. Kulshreshta, Nanotechn. **17**, 1278 (2006).
[14] H. Saekl, H. Tabata, T. Kawai, Solid State Commu. **120**, 439(2001).
[15] H. Schmidt, N. Diaconu, H. Hochmuth, Z. M. Lorenz, E. Squinazi, A. Poppl, D. Spemann, K.W. Nielsen, R. Gross, G. Wanger, M. Grundma, Super Latt. Microstruct. **39,** 334 (2006).
[16] T. Fukumura, Z. Jin, M. Kawasaki, T. Shono, T. Hasegawa, S. Koshihara, H. Koinuma Appl. Phys. Lett. **78**, 2700 (2001).
[17] J. H. Shim, T. H. Wang, S. Lee, J. H. Park, S.J. Han, Y.H. Jeong, Appl. Phys. Lett. **86** 082503 (2005).
[18] S.J. Han, J. W. Song, C. H. Yang, J. H. Park, Y. H. Jeong, K.W. Rhie, Appl. Phys. Lett. **81**, 4212(2002).
[19] Jung S W, An S J, Yi GC, Jung CU, Lee SI, Chos Appl. Phys. Lett. **80,** 4561(2002).
[20] A. K. Singh & Vijay S. Raykar, , Colloid Polym. Sci. **286**, 1667(2008).
[21] A. K. Singh, Adv. Powder Technol., doi:10.1016/j.apt.2010.02.002
[22] L.E. Brus, J. Phys. Chem. **90,** 2555(1986).
[23] A.K. Singh, V. Viswanath, V.C. Janu, J. Lumin. **129,** 874 (2009).
[24] C. Ronning P. X. Gao, Y. Ding, and Z. L. Wang, Appl. Phys. Lett. **84**(5) 783 (2004).
[25] F. Zhu, Y. Zhang, Y. Yan, W. Song, L. Xia, Sci., **31**(2), 121 (2008).
[26] S. Norberg, K. R. Kittilstved, J. E. Amonette, R.K. Kukkadapu, D.A. Schwartz, D,R. Gamelin, J. Am. Chem. Soc. **126,** 9387(2004).
[27] P. V. Radovanovic, D. R. Gamelin, Phy. Rev. Lett. **91,** 157202-3(2003).

*Corresponding author: draksingh@hotmail.com; aksingh@hotmail.com